

MOTRING REGIME CONTROL OF AN INTERIOR PERMANENT MAGNET SYNCHRONOUS MACHINE

Dorin LUCACHE, Vasile HORGA, Marcel RĂŢOI,
Alecsandru SIMION, Mihai ALBU

"Gh.Asachi" Technical University of Iasi
Blvd. Mangeron 53, RO-700050 Iasi
lukake@tuiasi.ro, horga@tuiasi.ro, ratoi@tuiasi.ro, asimion@ee.tuiasi.ro

Abstract – The interior permanent magnet synchronous machines (IPMSM) have several desirable features for automotive application, when are expected to operate at every load point inside the envelope as defined the maximum torque-speed curve. The paper presents a control structure of an interior permanent-magnet synchronous machine in the motoring regime over a wide speed-range. Experimental test results are shown and analyzed.

Keywords: interior permanent – magnet synchronous machine, vector control, flux weakening.

1. INTRODUCTION

The continuous cost reduction of magnetic materials with high energy density and coercitivity led to consider the permanent magnet (PM) synchronous machines as high attractive candidates both in automotive, tools machines and residential drive applications.

The interior (or buried) permanent magnet (IPM) motors due to their saliency develop supplementary reluctance torque and thus present a higher torque capability than the surface-mounted permanent magnet (SPM) motors. This is why the IPM synchronous machine (IPMSM) is an attractive solution for an integrated starter-generator (ISG). The main requirements of the ISG control are to ensure the necessary high torque as starter and the constant output voltage and frequency, irrespective of the input speed and load, as generator.

In the paper, the IPMSM was considered playing the role of an automotive starter. The used control algorithm is a combination of some techniques found in the literature and is based on the maximum torque-per-ampere strategy (minimum copper loss). A prototype system was tested in order to confirm the control algorithms and dSPACE based experimental results are presented and discussed.

2. MATHEMATICAL MODEL

In the d - q axis synchronous frame, the dynamic equations of the IPMSM can be expressed as:

$$\begin{cases} u_{sd} = R_s i_{sd} + L_d \frac{di_{sd}}{dt} - \omega_e L_q i_{sq} \\ u_{sq} = R_s i_{sq} + L_q \frac{di_{sq}}{dt} + \omega_e L_d i_{sd} + \omega_e \psi_m \end{cases} \quad (1)$$

Symbols u and i denote voltage and current, ψ_m the flux linkage of the permanent magnets in the d -axis rotor, L_d is the d -axis self-inductance, L_q is the q -axis self-inductance, ω_e is the electrical speed, respectively, and index s denotes parameters and variables associated with stator.

The developed electromagnetic torque t_e in terms of stator currents is expressed as:

$$t_e = p[\psi_m i_{sq} - (L_q - L_d) i_{sd} i_{sq}] \quad (2)$$

where p denotes the number of pole pairs. This has two components: the alignment torque produced by the flux linkage and the reluctance torque produced by the saliency. It is desirable that the reluctance torque should be properly utilized in order to increase the whole efficiency of the IPMSM drives.

At the low speed, the back-electromotive force is small and so there is enough voltage to control the current to generate the torque. As the rotor speed increases, the marginal voltage to control the current is decreased and the torque becomes highly distorted so the flux weakening method should be applied [1].

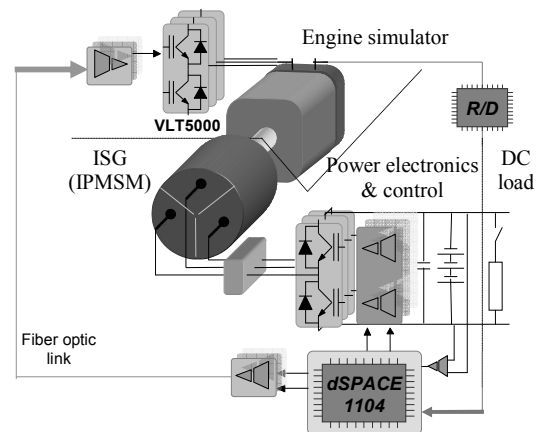


Fig.1 Experimental setup

The extension range of the speed is solely limited by the structure and the parameters of the motors under the given condition of voltage and current limitation. The maximum voltage $U_{s\ max}$ that the inverter can supply the machine is limited by DC link voltage and PWM strategy. When the voltage space vector strategy is used, $U_{s\ max} = U_{DC} / \sqrt{3}$. Also the maximum current $I_{s\ max}$ is determined by the inverter current rating and machine thermal rating. So, the imposed limits for the motor's voltage and current are:

$$\begin{cases} u_{sd}^2 + u_{sq}^2 \leq U_{s\ max}^2 \\ i_{sd}^2 + i_{sq}^2 \leq I_{s\ max}^2 \end{cases} \quad (3)$$

Neglecting the stator resistance (when speed increases the term ω_e becomes more important), from (1) the steady-state voltage limit equation yields:

$$\left(i_{sd} + \frac{\Psi_m}{L_d} \right)^2 \left(\frac{L_d}{L_q} \right)^2 + (i_{sq})^2 \leq \left(\frac{U_{s\ max}}{\omega_e L_q} \right)^2 \quad (4)$$

From (3) and (4) it can be seen that the current limit equation determines a circle with a radius of $I_{s\ max}$, while the voltage limit equation determines a series of nested ellipses (for the IPMSM, $L_q > L_d$). Fig.2 shows the current-limit circle and the voltage-limit ellipses in the i_{sd} - i_{sq} plane.

The voltage-limit ellipse decreases as the speed increases. At a so-called base speed ω_{base} , the maximum torque point A is on the cross point of maximum torque-per-current trajectory and current-limit circle. When the IPMSM is operated from the start up to the base speed in the constant torque region, the voltage-limit ellipse exceeds the maximum current boundary and no voltage limitation needs to be considered in this situation.

But beyond the base speed, the IPMSM cannot be operated without flux-weakening control and so, to extend the speed range, a proper demagnetizing current has to be applied depending on the operating speed. The current vector trajectory will move along the boundary of the current-limit circle (from A to B in Fig.2) as rotor speed increases.

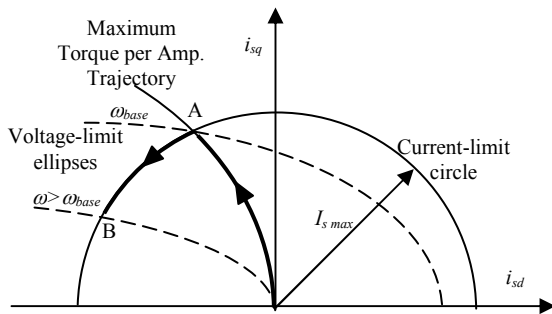


Fig.2 Current-limit circle and voltage-limit ellipses in the i_{sd} - i_{sq} plane

Without a proper flux weakening at higher speed, the current regulators would be saturated and lose their controllability. Since the onset of current regulator saturation varies according to the load conditions and the machine parameters, the beginning point of the flux weakening should be varied. The late starting of the flux weakening may result in undesired output torque drop, but the early starting deteriorates the acceleration performance [2].

3. CONTROL STRUCTURE

As opposed to SPMSM, the $i_d=0$ control method is not suitable for the IPM synchronous machines because the reluctance torque is not produced even if this kind of machine have a saliency.

At low speeds, because the absence of voltage limitation, the current vector might be controlled to fully use reluctance torque in order to maximize the machine efficiency. Typically, it is chosen to maximize the torque per amp ratio by controlling the current vector in order to have an optimum inclination versus q-axis. In order to get the maximum torque control, the inclination angle γ of the current vector (Fig.3) depends on the load conditions, taking values between 0 and 45° [3].

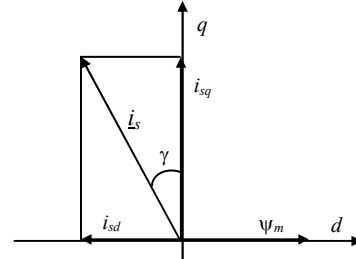


Fig.3 Current phasor diagram in the d - q frame

The maximum torque-per-ampere strategy seeks to get a certain torque with the smallest possible stator current amplitude (so with minimum copper loss). Because $i_{sd} = -i_s \sin \gamma$ and $i_{sq} = i_s \cos \gamma$, where

$$i_s = |i_s|, \quad (2) \text{ becomes:}$$

$$t_e = p \left[\Psi_m i_s \cos \gamma + \frac{1}{2} (L_q - L_d) i_s^2 \sin 2\gamma \right] \quad (5)$$

and imposing the condition :

$$dt_e / d\gamma = 0 \quad (6)$$

the relation between i_{sd} and i_{sq} for the maximum torque per ampere control is derived as

$$i_{sd} = \frac{\Psi_m}{2(L_q - L_d)} - \sqrt{\frac{\Psi_m^2}{4(L_q - L_d)^2} + i_{sq}^2} \quad (7)$$

This relation is shown as the maximum torque-per-

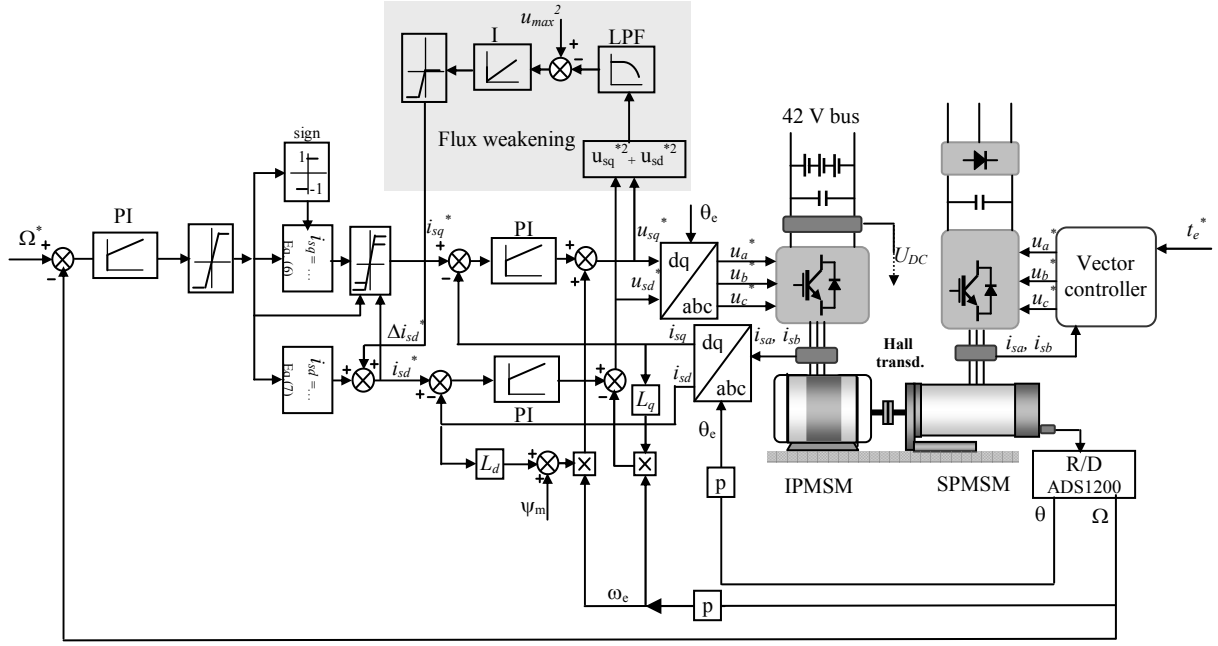


Fig.4 Implemented control system

ampere trajectory in Fig.2.

This relation is shown as the maximum torque-per-ampere trajectory in Fig.2.

Above the base speed, the normal operation is possible only applying the flux weakening and the maximum torque is obtained when the drive operates in the voltage and current limits. The flux weakening control of PM synchronous machines is conducted by injecting the d -axis current i_{sd} negatively, which is different from induction machine where the flux is weakened by decreasing the d -axis current.

The proposed control scheme in Fig.4 is a combination of the previous discussed techniques.

Two PI controllers, implemented in the synchronous reference frame, are used for the current control, followed by a decoupling circuit. In the constant power operation, a closed-loop voltage control is used to ensure an automatically onset of the accurate flux-weakening operation, depending on the load condition and machine parameters. Flux weakening mode is entered when the error

$$\varepsilon = u_{smax}^2 - (u_{sd}^2 + u_{sq}^2) < 0 \quad (8)$$

becomes negative. This error, passing through a low-pass filter (LPF) and regulated by an I controller, lead to the d -axis current increases toward the negative direction to prevent saturation of the current regulators. The I controller output is limited (to avoid irreversible demagnetization) so that the d -axis current to be between 0 and the minimal allowable $i_{sd}^* = -I_{sdmax}$.

The magnitude of the injected stator current i_s can be expressed as

$$i_s = \sqrt{i_{sd}^2 + i_{sq}^2} \quad (9)$$

and taking into account (2), the d - q axis components of the current vector that ensures the maximum torque-per-ampere yields

$$i_{sq} = \text{sign}(i_s) \cdot \sqrt{i_s^2 - i_{sd}^2} \quad (10)$$

where

$$i_{sd} = \frac{\Psi_m - \sqrt{\Psi_m^2 + 8(L_q - L_d)^2 i_s^2}}{4(L_q - L_d)} \quad (11)$$

The last equation is equivalent with (7) but expressing the d -axis current as a function of i_s , taking into account (9).

Thus, when the d -axis current is increased with respect to the voltage limit, the q -axis current is depressed in order to ensure the current limit condition. More, a saturation block with adaptive limits take into account the flux weakening command Δi_{sd}^* and forces ones more the operating point to not exceed the current-limit circle. In this way the current regulators regain the ability of regulating the d -axis and q -axis currents and the maximum torque-per-ampere is produced at the crossing point between the current limit circle and voltage limit ellipse, in the constant power region.

Because this scheme utilizes for flux weakening the output voltage of the PI current regulators and the outer voltage-regulating loop instead of the IPM synchronous machine model, it becomes robust and insensitive to load conditions and load parameters.

3. EXPERIMENTAL RESULTS

In this paper a commercial IPMSM, operating at low voltage and high currents, was used (rated parameters in Table 1). This is mechanical coupled to an internal combustion engine simulator that consists in a SPMSM (1.9 kW, 330V, 4.4A and 4000rpm). The speed of the engine simulator can be varied in closed loop by means of its own inverter. Though the obtained speed characteristics may be different from a real engine, this experimental setup allows testing the validity of the proposed control algorithms successfully [12].

Rated power [kW]	4
Peak current constraint [A]	160
Number of phases	3
Number of poles	12
R_s [m Ω]	21
L_d [mH]	0.076
L_q [mH]	0.12
Ψ_m [Wb]	0.009
Rated speed [rpm]	2000
Rated phase voltage [V]	11

Table 1: IPM synchronous machine characteristics

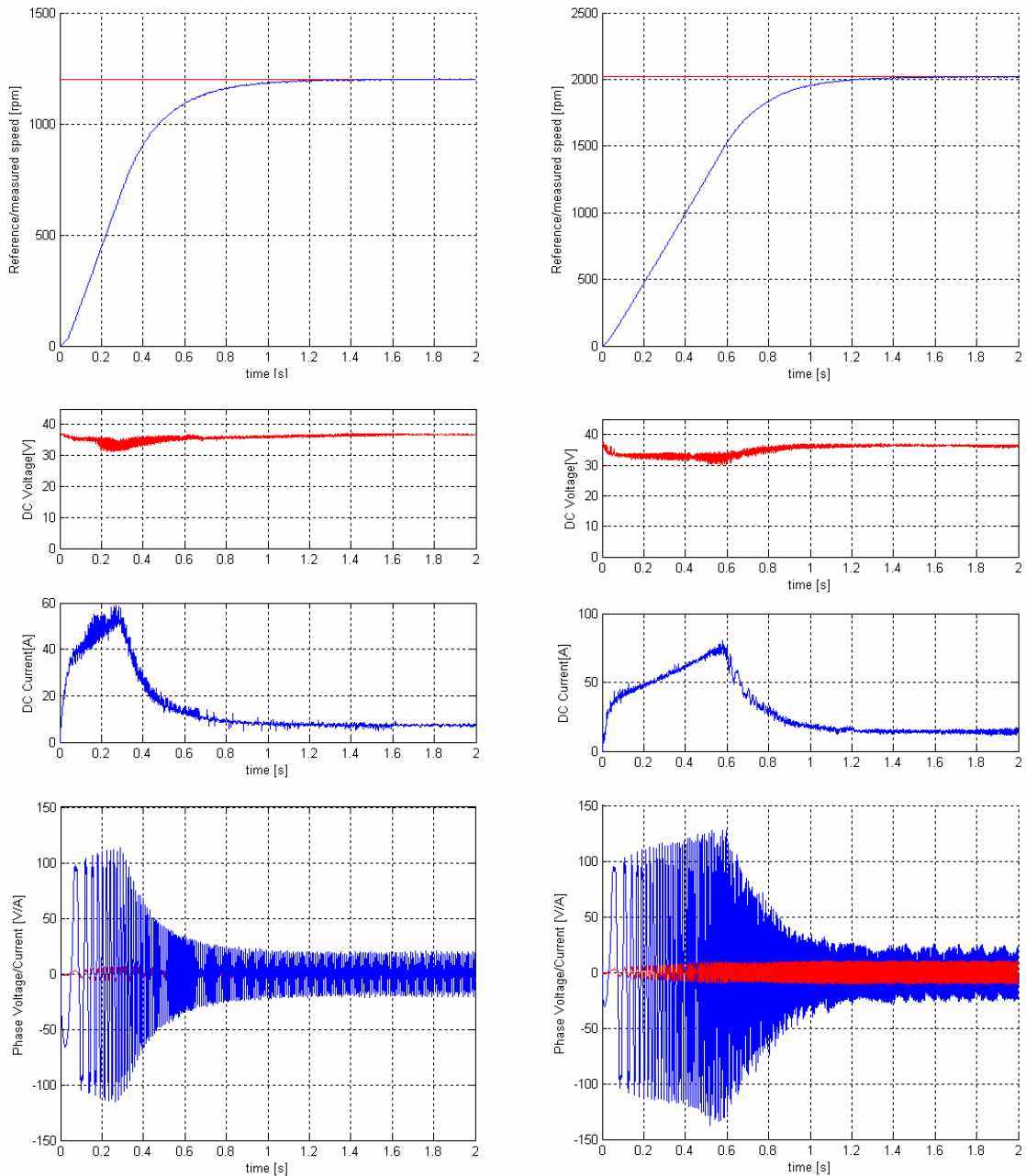


Fig.5 Experimental results below (left side) and above (right side) the base speed

To control the whole system, a dSPACE 1104 board and ControlDesk software is being used. The external lead-acid battery pack is the supply source for the IPMSM in the motoring regime. A capacitive filter is connected to the DC line.

The following figures present the experimental results for a time interval of two seconds when the IPMSM operates as motor below and above the base speed.

A special attention was paid to handle the non-sinusoidal currents produced by the IPMSM due to its specific geometry and construction, as seen in Fig.6. The current and voltage space phasor loci in the stationary reference frame presented in Fig.7 confirm the presence of the fifth harmonic in the phase current of the IPMSM [13]. These currents are acquired and used to generate the reference voltage commands and consequently these present many oscillations, as we can see in Fig.9.

The tested system presents good dynamic performances and responds well also in more complex situations.

4. CONCLUSIONS

This paper proposes a control solution for an IPMSM applying the vector control in the motoring regime. The experimental results confirm a very good behavior both in constant torque region and the constant power region.

References

- [1] J. H. Song, J. M. Kim, and S. K. Sul, "A new robust SPMSM control to parameter variations in flux weakening region," *IEEE IECON*, vol. 2, pp. 1193-1198, 1996.
- [2] Y. S. Kim, Y. K. Choi and J. H. Lee, "Speed-sensorless vector control for permanent-magnet synchronous motors based on instantaneous reactive power in the wide-speed region," *IEE Proc-Electr. Power Appl.*, vol. 152, No. 5, pp. 1343-1349, Sept. 2005.
- [3] S. Morimoto, M. Sanada and K. Takeda, "Wide-speed operation of interior permanent magnet synchronous motors with highperformance current regulator," *IEEE Trans. Ind. Applicat.*, vol. 30, pp. 920-926, July/Aug. 1994.
- [4] N.Bianchi, S.Bolognani, High-performance PM synchronous motor drive for an electrical scooter, *IEEE Trans. on Industry Applications*, vol.37, no.5, Sept./Oct.2001, pp.1348-1355
- [5] D. S. Maric, S. Hiti et al., "Two flux weakening schemes for surfacemounted permanent-magnet synchronous drives. Design and transient response considerations," in *Proc. ISIE*, 1999, pp. 673-678.

- [6] C-T. Pan, S-M. Sue, A linear maximum per ampere control for IPMSM drives over full-speed range, *IEEE Trans. on Energy Conv.*, Vol.20, No.2, June 2005, pp.359-366
- [7] J.L.Shi, T.H.Liu, S.H.Yang, Nonlinear controller design for an interior permanent-magnet synchronous motor including field weakening operation, *IET Electr. Power Appl.*, Vol.1, No.1. January 2007, pp. 119-126
- [8] J. M. Kim and S. K. Sul, "Speed control of

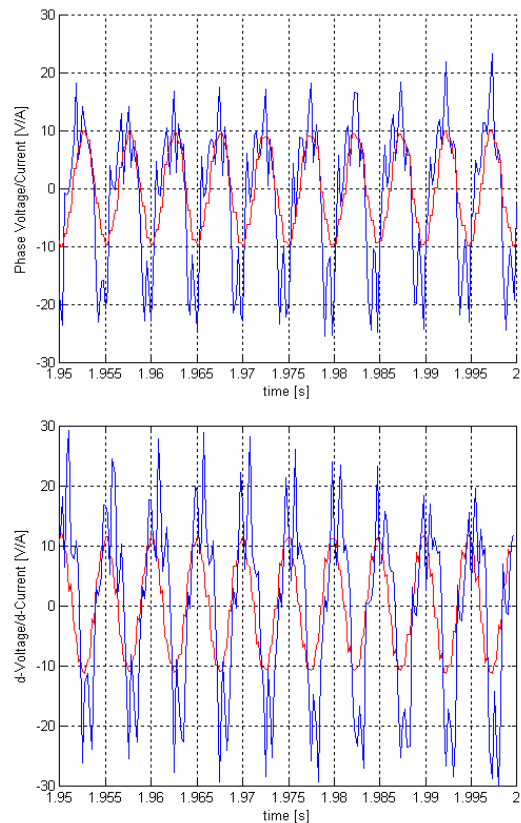


Fig.6 The phase- and d -axis voltage and currents

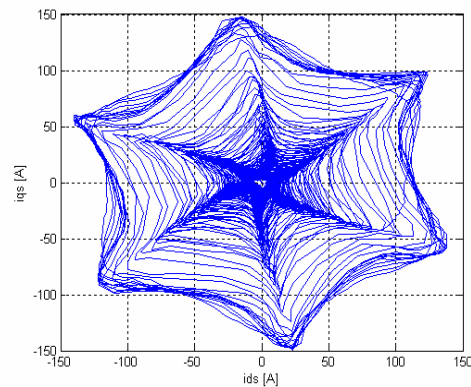


Fig.7 Current space phasor loci in the stationary reference frame below the base speed

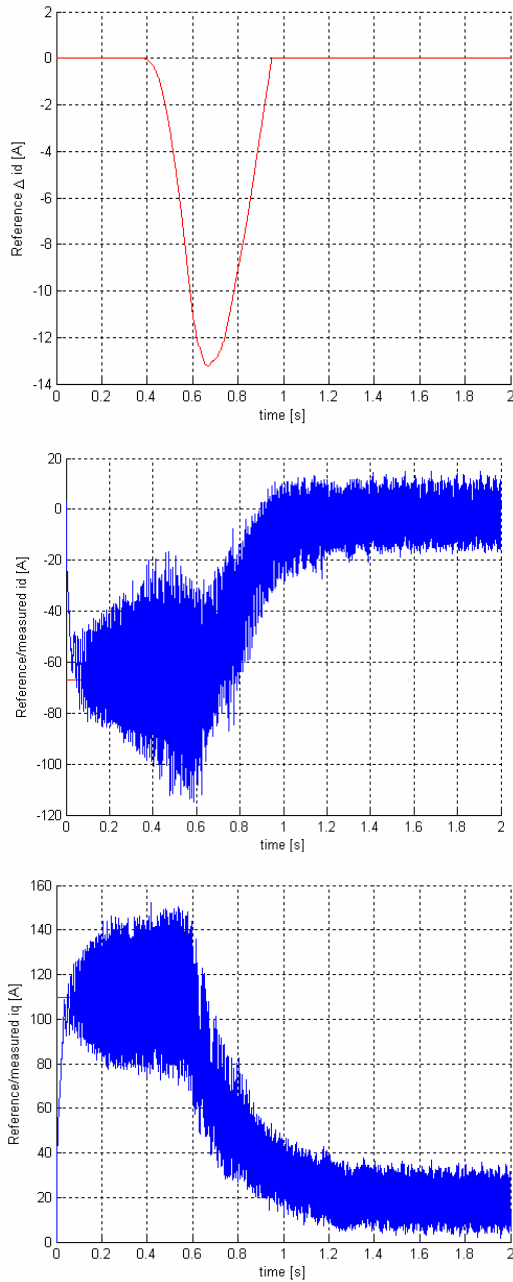


Fig.8 Reference voltage commands in the constant power region

interior permanent magnet synchronous motor drive for the flux weakening operation," *IEEE Trans. Ind. Applicat.*, vol. 33, pp. 43-48, Jan./Feb. 1997.

- [9] T. M. Jahns and V. Blasko, "Recent advances in power electronics technology for industrial and traction machine drives," *Proc.IEEE*, vol. 89, pp. 963-975, June 2001.
- [10] Thomas M. Jahns, "Motion control with permanent-magnet ac machines," in *Proc. IEEE*, vol. 82, Aug. 1994, pp. 1241-1252.
- [11] S.Shinnaka, T. Sagawa, New optimal control current methods for energy efficient and wide speed-range operation of hybrid-field synchronous motor, *IEEE International Conference on Electric Machines and Drives*, May 2005, pp. 535 - 542
- [12] D.Lucache, V.Horga, M.Albu, M.Ratoi, Indirect Field Oriented Control of an Integrated Starter Generator, *Proceedings of IEEE Industrial Electronics Conference IECON2006*, November 7-10, 2006, Paris, France, pp.5107-5112
- [13] P. Vas, *Parameter Estimation, Condition Monitoring, and Diagnosis of Electrical Machines*, Clarendon Press, Oxford, 1993
- [14] dSPACE 1104 Users's Guide, Version 4.2, dSPACE GmbH